

# New solvating cross-linked polyether for lithium batteries

F. Alloin, J-Y. Sanchez, M. Armand

*Laboratoire d'Ionique et d'Electrochimie des Solides, Domaine Universitaire, BP 75, 38402 Saint-Martin-d'Hères Cedex, France*

---

## Abstract

A new attractive polycondensation provides cross-linked solvating polyethers. The electrolytes prepared from these networks exhibit good ionic conductivities from ambient temperature. Their thermal and electrochemical behaviour allow their use in lithium batteries. A comparison between the conductivities of lithium, sodium and potassium network electrolytes shows that lithium electrolytes are more conductive at high concentration while for O/M > 20 potassium electrolytes exhibits the best conductivity.

**Keywords:** Polycondensation; Polymer electrolytes; Ionic conductivity; Poly(oxyethylene) network; Lithium batteries

---

## 1. Introduction

Polymer electrolytes are of current interest for the development of advanced, high-energy storage electrochemical devices. Safety, long lifetime and absence of self-discharge have already been established for ACEP<sup>1</sup> lithium batteries. Owing to its high solvating ability as well as to its electrochemical, thermal and mechanical stabilities, high molecular weight poly(oxyethylene) (POE) has been investigated extensively as host polymer. Thus, most common polymer/salt complexes have been based on POE 'immobile solvent' [1]. However, this semi-crystalline polyether leads to partially crystalline polymer-salt complexes at room temperature, which lowers the ionic conductivity. Indeed, ten years ago [2], <sup>7</sup>Li NMR performed on semi-crystalline POE/lithium salt complexes established the prevalence of the ionic conductivity in the amorphous phase. One way to remove the crystallinity induced by the oxyethylene unit repetition consists in preparing comb-shaped polymers in which the solvating properties are provided by short POE chains attached, as hanging side groups, to a supporting polymer backbone. If the oligo(oxyethylene) size is kept short, the polymer remains amorphous and this strategy has therefore been used by several groups who prepared comb-shaped structures based on poly(methacrylate) [3,4], poly(itaconate)

[5–10], poly(phosphazene) [11,12] or poly(siloxanes). Polycondensation of  $\alpha,\omega$ -dihydroxy oligo(oxyethylene), whose trade name is polyethylene glycol PEG, with di- or triisocyanate gives linear or tridimensional polycondensates and allows amorphous materials to be obtained [13,14]. As an alternative to polyether solvating units, other solvating functions such as 16-crown-5-ether units [15–17] have also been grafted on to a poly(phosphazene) skeleton. Nevertheless the electrochemical stability of these esters, siloxane or urethane links versus lithium metal, is questionable.

On the contrary, by polycondensation between oligo poly(ethylene glycol) and CH<sub>2</sub>Cl<sub>2</sub>, Craven et al. [18,19] suggested a clever route to reduce the crystallinity content in polyethers, without compromising the electrochemical stability. Unfortunately, though these polyethers, in which short oxyethylene blocks are linked by oxymethylene units, exhibit rather high conductivities, their poor mechanical properties, as well as the acetal link sensitivity to acid traces should not favour industrial scale-up.

Using the Williamson reaction, we have investigated the polycondensation between several polyethylene glycol and unsaturated dihalide compounds such as 3-chloro-2-chloromethyl-1-propene [20,21].

## 2. Experimental

### 2.1. Polycondensation reaction

The polycondensates were prepared using poly(ethylene glycol), PEG-400, PEG-1000, PEG-2000,

---

<sup>1</sup> ACEP: 'Accumulateur à Electrolyte Polymère', International programme between Hydro-Quebec from Canada, INPG and CNRS from France.

and 3-chloro-2-chloromethyl-1-propene from Aldrich, used as-received [20,21].

## 2.2. Network formation

Film cross-linking is induced by free-radical polymerization, using dibenzoyl peroxide as initiator. One hour heating (70 °C) of the membrane, followed by a thorough washing in methanol to remove non-cross-linked chains allows between 90 to 95% of insoluble material to be recovered. A comparative attempt using soxhlet extraction gave approximately the same yield. Network polymer electrolytes, abbreviated to NPC, were obtained by swelling the film with a salt solution in acetonitrile. After the solvent removal, the weight difference of the membranes makes it possible to determine the salt concentration.

## 2.3. Thermal analysis

Differential scanning calorimetry (DSC) analyses were performed in helium on a Netzsch STA409 thermal analyser. Samples were first cooled down to –100 °C, then heated at 10 °C min<sup>–1</sup> up to 150 °C. Although the first scan gave an irregular thermogram it allows the sample to be characterized without modifying the crystallinity content. The samples are again cooled down at –100 °C and then heated at 10 °C min<sup>–1</sup> to 150 °C. The second scan allows generally a better determination of the glass-transition temperature (*T<sub>g</sub>*).

Thermogravimetric analyses (TGA) were either performed in helium or in air. The samples were first heated from room temperature up to polymer degradation at a 10 °C min<sup>–1</sup> heating rate. In another way the sample is kept, either in air or in helium, in isothermal condition while the weight loss is recorded.

## 2.4. Electrochemical measurements

A.c. conductivity measurements were carried out under vacuum using a HP4192A impedance analyser, from room temperature up to 90 °C, over the frequency range 5 Hz–10 MHz. The samples were sandwiched between two stainless-steel electrodes. The conductivity was measured at various temperatures, after an equilibrium time of one hour at each temperature.

## 2.5. Cyclic voltammetry

The electrochemical stability was checked by cyclic voltammetry using microelectrodes. The scanning rate used was 6 mV s<sup>–1</sup> and all the voltammograms were performed at 80 °C. At this temperature all samples are amorphous and exhibit a conductivity close to 10<sup>–3</sup> S cm<sup>–1</sup>.

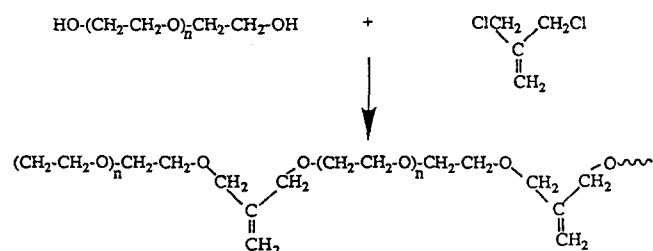
## 2.6. Salt synthesis

The salt, lithium bis(trifluoromethyl sulfonyl) imide, Li(CF<sub>3</sub>SO<sub>2</sub>)<sub>2</sub>N–LiTFSI—was obtained by commercial source, while the other salts were synthesized from exchange reaction between LiTFSI and M<sub>2</sub>CO<sub>3</sub>, (M = K and Na, in tetrahydrofuran (THF) for several hours. According to elementary analysis, the alkaline exchange yield is quantitative.

## 3. Results and discussion

### 3.1. Polycondensation

We have investigated the polycondensation between PEG-400, PEG-1000, PEG-2000, and 3-chloro-2-chloromethyl-1-propene. Due to its leaving-group effectiveness the dihalide alkene undergoes a fast polycondensation at moderate temperature ranging from 35 to 45 °C. The reaction, carried out either in acetonitrile or in molten polyethylene glycol, is described as follows:



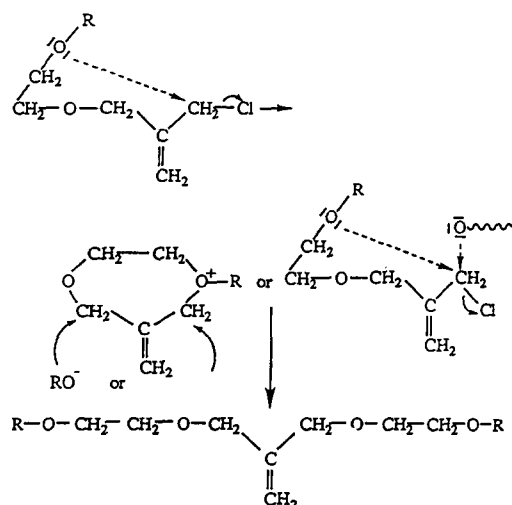
A kinetic study of the condensation reaction, performed on model alcohol molecules such as ethanol and methoxyethanol in acetonitrile, enabling nucleophilic substitution to occur but forbidding polycondensation, showed the importance of the  $\beta$ -ether function on the reaction rate. Indeed the reaction is completed in 4 h at 25 °C when using methoxyethanol, while the yield reaches only 50% after 50 h when using ethanol. Moreover, the reaction rate enhancement of the second chloride substitution with respect to the first one, suggested an anchimeric assistance by the  $\beta$ -ether function, according to Scheme 1.

The main consequence of this mechanism is that a slight dichloride excess, with respect to the OH end functions, does not result in a marked decrease of the average polymerization degree  $\overline{DP}_n$ .

### 3.2. Physico-chemical characterizations of the polycondensates and networks

#### 3.2.1. Molecular weight determination

Gel permeation chromatography (GPC), performed on the crude samples, allows the total consumption of the initial reactants to be checked, namely the dichloride alkene and the PEG-1000, and does not reveal any



Scheme 1. Anchimeric assistance.

Table 1

Average molecular weights of polycondensate 1000 in polystyrene equivalents

PEG (g/mol)	1000
$\overline{M}_n$ (g/mol) GPC	47000
$\overline{M}_w$ (g/mol) GPC	105000
$I = \overline{M}_w / \overline{M}_n$	2.2
% function consumption	98.9

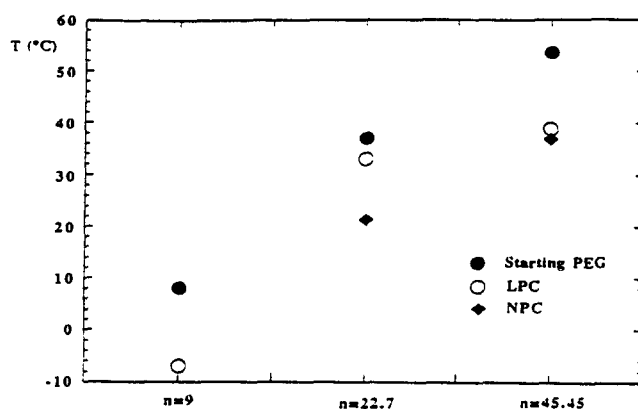
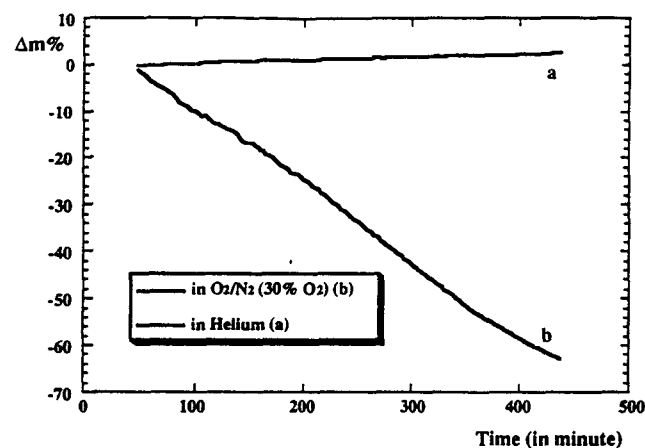
oligomers traces. The sample characterizations are summarized in Table 1. After cross-linking, the soluble materials recovered either by washing or by soxhlet extraction range from 5 to 10% in weight. GPC analysis of these soluble polymers show that they are not dimers but rather medium weight polymers.

### 3.2.2. Differential scanning calorimetry analyses

The incorporation of the isobutenyl links between the solvating oligo(oxyethylene) blocks, then the polycondensate cross-linking, markedly decreases the crystallinity content. It thus drops from 75% in PEG-1000 to 56% in Polycondensate 1000 and to 34% in NPC1000. The melting points ( $T_m$ ) evolution from PEG to polycondensate and network versus the solvating block length PEG-400 ( $n=9$ ), PEG-1000 ( $n=22.7$ ) and PEG-2000 ( $n=45.45$ ), is given in Fig. 1. The sharp  $T_m$  decrease from PEG to the networks confirms the previous observation concerning the trend of the crystallinity content.

### 3.2.3. Thermogravimetric analyses

Among the specifications that large batteries must meet, notably for application in electrical cars, safety is probably the main requirement. Indeed a 40 kWh electrical car, should at least carry about 300 kg batteries. Thus, in the event of short-circuit, even for non-lithium

Fig. 1. Melting point evolution from PEG to polycondensate and network;  $n$  = solvating block motif number.Fig. 2. Thermal stability for the network NPC1000: (a) isotherm, 250 °C in helium, and (b) isotherm, 250 °C in  $O_2/N_2$  (30%  $O_2$ ).

batteries, the dramatic temperature increase may lead to a battery explosion. The resort to all-solid components enables indisputably the batteries to be safer, as no volatile products may increase the internal pressure of the cell. Thus, two years ago, in Münster [22], Hydro-Quebec presented a short-circuit test performed on a 10 Wh cell. In the cell voltage and temperature evolution three stages must be discerned:

- first the cell voltage drops sharply, while the temperature cell increases;
- the temperature reaches 200 °C and then exceeds the melting temperature of the metallic lithium, and
- even in contact with liquid lithium, no exothermic event is recorded.

In order to check the thermal stability of the network we first performed a TGA in helium from room temperature at 10 K min<sup>-1</sup> heating rate. The thermogram shows that weight loss starts as from 300 °C. Nevertheless, scanning TGA is a flattering analysis for any sample. Therefore, we submitted this network to an isothermal treatment at 250 °C in helium and in a mixture  $O_2/N_2$  with 30%  $O_2$ . Fig. 2 exhibits a long-term stability of the network in helium, as no weight

loss occurred after 7 h. On the contrary, a thermal degradation occurs in oxygen with a weight loss rate of about 9% per hour. This result is very impressive as it means that, even at a temperature kept at about 60 °C above the lithium melting point and in a gaseous mixture enriched with oxygen, the weight loss in the first hour is only 9%.

### 3.2.4. Electrochemical behaviour

The ionic behaviour of polymer electrolytes, prepared from the dissolution of three trifluoromethyl sulfonyl imide alkaline salts  $(CF_3SO_2)_2N^-M^+$  with  $M=Li^+$ ,  $Na^+$  and  $K^+$  in these networks were investigated. We abbreviated the salts as MTFSI and the host-solvating networks as NPC. Fig. 3 displays the temperature dependence of the conductivity for various NPC1000/LiTFSI compositions. High conductivities of a non-plasticized polymer electrolyte of several compositions, were obtained at room temperature, the best one, O/Li=9, reaching  $2 \times 10^{-5} \text{ S cm}^{-1}$  at 20 °C.

The Arrhenius conductivity plots of KTFSI (Fig. 4) exhibit a free-volume-type behaviour. Contrary to

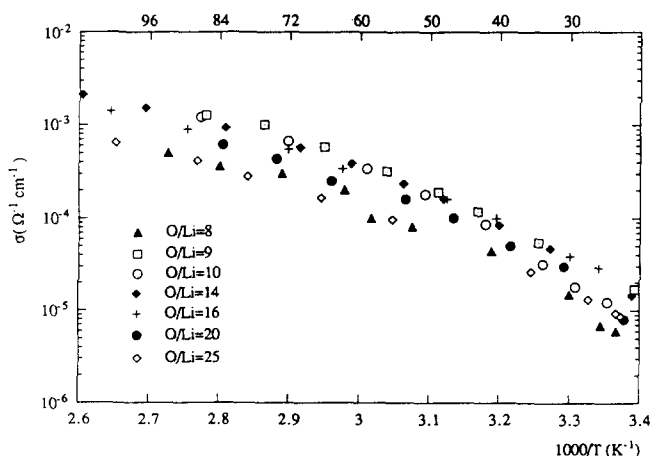


Fig. 3. Conductivity vs.  $T^{-1}$  for NPC1000/LiTFSI complexes at various salt concentrations.

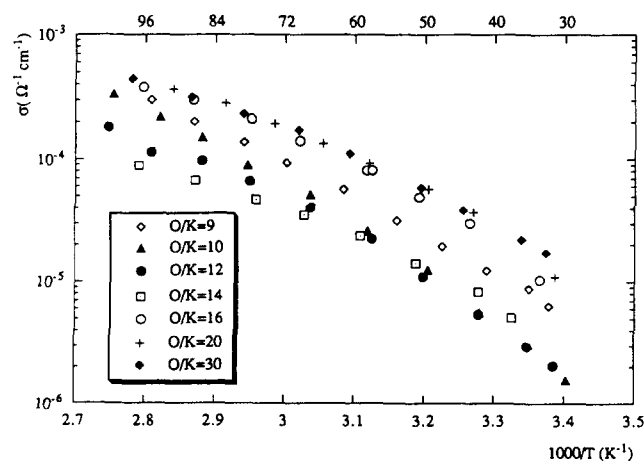


Fig. 4. Conductivity vs.  $T^{-1}$  for complex NPC1000/KTFSI.

NPC1000/LiTFSI, the best conductivities were obtained for low salt concentrations  $O/K > 14$ , with  $10^{-5} \text{ S cm}^{-1}$  at 20 °C for  $O/K=30$ . The same behaviour is observed for the complexes NPC1000/NaTFSI (Fig. 5), where the best conductivity is observed for  $O/Na=20$ .

Fig. 6 shows a comparison of the Arrhenius plots of most conductive complexes of each salt. As shown by these plots, the values are almost similar at room temperature, while LiTFSI complex is 50% more conductive than the NaTFSI one, and twice as much as the KTFSI one, at 80 °C. The conductivity isotherms versus salt concentration are represented in Fig. 7, at 50 °C, for the different salts. At high concentrations, the complexes NPC1000/LiTFSI showed the best conductivities with almost one order of magnitude between lithium and potassium salts, NPC1000/NaTFSI conductivities ranging between lithium and potassium electrolytes. Whatever the alkaline cation, the conductivities are the same for the concentration  $O/M=20$ , whereas for more diluted solutions the electrolyte conductivities decrease according to  $\sigma_{K^+} > \sigma_{Na^+} > \sigma_{Li^+}$ .

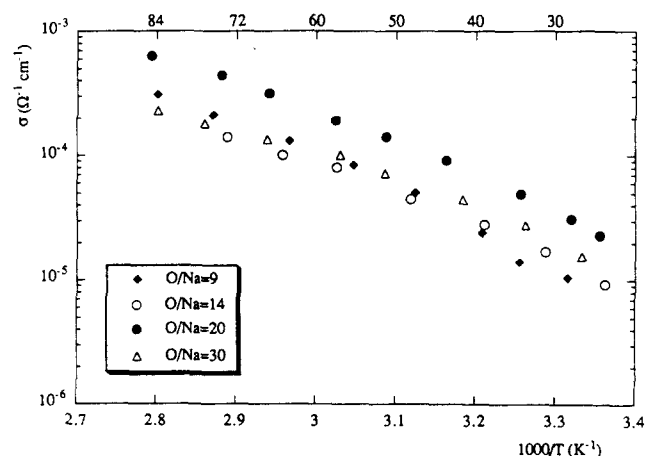


Fig. 5. Conductivity vs.  $T^{-1}$  for complex NPC1000/NaTFSI.

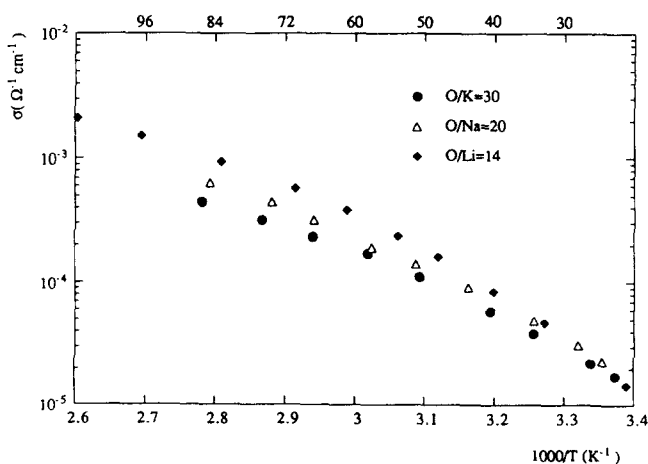


Fig. 6. Comparison of best conductivity levels for several NPC1000/salt complexes.

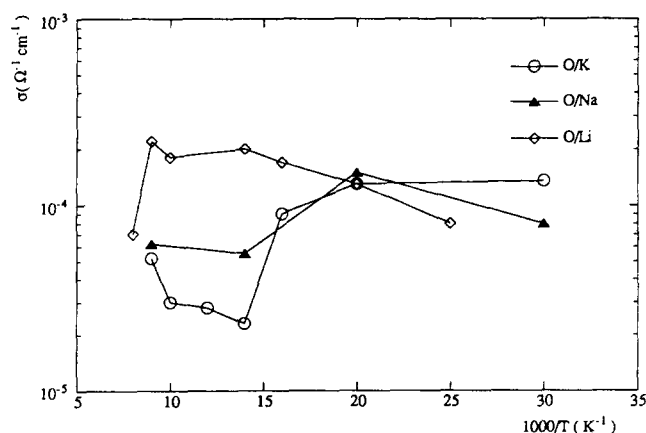


Fig. 7. Comparison of conductivity isotherms of the three complexes NPC1000/MTFSI for all salt concentrations,  $T = 50\text{ }^{\circ}\text{C}$ .

Table 2

Melting point ( $T_m$ ) and glass-transition temperature ( $T_g$ ) vs. salt concentration of several NPC1000/salt complexes

O/Li	LiTFSI		NaTFSI		KTFSI	
	$T_g$	$T_m$	$T_g$	$T_m$	$T_g$	$T_m$
2	-19.8		-2.4		-20	
10	-38		-45.1		-40	
12	-42				-48.2	
14	-43.5		-54.7			
16	-46.9				-55	3.4
20	-51.5	-4.1	-56.8	7.4	-55.9	10
25	-52.1	10.6				
30			-56.5	12.7	-59.4	16.6

Discrepancies in salt dissociation as well as in cation and chain mobilities lead one to comment on the different behaviour of the three salts. Despite the fact that the diluted LiTFSI complexes are slightly less crystalline than the potassium and sodium complexes, all these NPC electrolytes are amorphous at ambient temperature. Nevertheless, the melting points ( $T_m$ ) remain lower than  $20\text{ }^{\circ}\text{C}$ . In amorphous polymers, chain mobility is closely related to the glass-transition temperature,  $T_g$ . From Table 2 we can see that, whatever the cation,  $T_g$  increases with the salt concentration. The  $T_g$  comparison shows that the reduced conductivities of sodium and potassium polymer electrolytes with respect to that of lithium cannot be connected to the chain mobility as, for the same concentration, the  $T_g$  of sodium and potassium electrolytes are lower than for the  $T_g$  of lithium. As the ionic character generally increases with the cation size, and as the lithium cation is not supposed to be more mobile than sodium and potassium cations the conductivity gap may be related to a prevalent anionic contribution in the lithium polymer electrolytes.

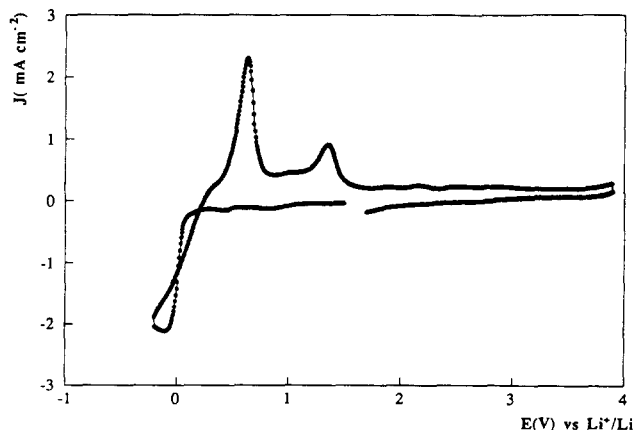


Fig. 8. Microvoltammetry performed on NPC1000/LiTFSI complex at  $80\text{ }^{\circ}\text{C}$ , platinum microelectrode  $\phi = 25\text{ }\mu\text{m}$ , scan rate  $= 6\text{ mV s}^{-1}$ .

### 3.2.5. Electrochemical stability

Cyclic voltammetries on microelectrodes were performed on a sample NPC1000/LiTFSI at  $80\text{ }^{\circ}\text{C}$ . Platinum microelectrode allowed the electrochemical stability in oxidation to be checked, whereas the reduction behaviour was investigated using a copper microelectrode. Fig. 8 shows the good electrochemical stability of our electrolyte at least up to 3.9 V. Though cyclic voltammetry is a useful tool to check the electrochemical stability of an electrolyte, this test is not enough reliable to check the electrolyte long-term stability in batteries, and the actual test remains the battery cycling. First attempts performed by Hydro-Quebec on the electrolyte NPC1000/LiTFSI exhibit good cycling efficiency.

## 4. Conclusions

Polycondensation of various types of polyethylene glycol with a dichloride alkylene lowers the crystallinity as well as the melting point of the resulting polycondensates, with respect to the high molecular weight of poly(oxyethylene) and polyethylene glycol. Free-radical initiators allows the cross-linking of the linear polycondensates, the resulting networks show high dimensional and thermal stabilities. Ambient temperature polymer electrolytes reaching a conductivity of  $2 \times 10^{-5}\text{ S cm}^{-1}$  at  $20\text{ }^{\circ}\text{C}$  were obtained by dissolution of alkaline imide salts MTFSI in the networks. According to these new polymers meeting the specifications for battery applications and to the synthesis requiring not any specific equipment, these polycondensates also appear good candidates for other applications in electrochemical devices such as electrochromic windows, sensors, etc.

## Acknowledgements

This work has been carried out with the financial support of Hydro-Quebec and the French Ministry of Research and Technology.

## References

- [1] M. Armand, Polymer electrolyte: the immobile solvent concept, in T. Takahashi (ed.), *Solids with High Conductivity*, World Scientific, Singapore, 1988.
- [2] C. Berthier, W. Gorecki, M. Minier, M. Armand, J.-Y. Chabagno and P. Rigaud, *Solid State Ionics*, **11** (1983) 91.
- [3] D.W. Xia, D. Soltz and J. Smid, *Solid State Ionics*, **14** (1984) 221.
- [4] D.J. Bannister, G.R. Davies, I.M. Ward and J.E. McIntyre, *Polymer*, **25** (1984) 1600.
- [5] J.M.G. Cowie and A.C.S. Martin, *Polym. Commun.*, **26** (1985) 298.
- [6] J.M.G. Cowie, R. Ferguson and A.C.S. Martin, *Polym. Commun.*, **28** (1987) 130.
- [7] J.M.G. Cowie and A.C.S. Martin, *Polymer*, **28** (1987) 627.
- [8] A.T. Anderson, M. Andrei, A.C.S. Martin and C. Robert, *Electrochim. Acta*, **37** (1992) 1539.
- [9] N. Kobayashi, M. Ushiyama and E. Tsuchida, *Solid State Ionics*, **17** (1989) 307.
- [10] J.M.G. Cowie, in J.R. MacCallum and C.A. Vincent (eds.), *Polymer Electrolyte Reviews*, Vol. 1, Elsevier Applied Science, Barking, UK, 1987.
- [11] P.M. Blonsky, D.F. Shiver, P. Austin and H.H. Allcock, *J. Am. Chem. Soc.*, **106** (1984) 6854.
- [12] D.F. Shriver, P.M. Blonsky, H.R. Allcock and P. Austin, *Solid State Ionics*, **18/19** (1986) 258.
- [13] A. Killis, J.-F. Le Nest, A. Gandini and H. Cheradame, *J. Polym. Sci.: Polym. Phys. Ed.*, **19** (1981) 1073.
- [14] H. Cheradame and J.-F. Le Nest, in J.R. MacCallum and C.A. Vincent (eds.), *Polymer Electrolyte Reviews*, Vol. 1, Elsevier Applied Science, Barking UK, 1987, p. 103.
- [15] J.M.G. Cowie and K. Sadaghianizadeh, *Polym. Commun.*, **29** (1988) 126.
- [16] J.M.G. Cowie and K. Sadaghianizadeh, *Makromol. Chem. Rapid Commun.*, **9** (1988) 387.
- [17] N. Andrei, J.M.G. Cowie and P. Prosperi, *Electrochim. Acta*, **37** (1992) 1545.
- [18] J.R. Craven, R.H. Mobbs, C. Booth and J.R.M. Giles, *Makromol. Chem. Rapid Commun.*, **7** (1986) 81.
- [19] J.R. Craven, C.V. Nicholas, R. Webster, D.J. Wilson, R.H. Mobbs, G.A. Morris, F. Heatley, C. Booth and J.R.M. Giles, *Br. Polym. J.*, **19** (1987) 509.
- [20] F. Alloin, J.-Y. Sanchez and M. Armand, *Solid State Ionics*, **60** (1993) 3.
- [21] F. Alloin, J.-Y. Sanchez and M. Armand, *J. Electrochem. Soc.*, **141** (1994) 1915.
- [22] Y. Choquette, M. Gauthier, A. Bélanger and B. Kapfer, *6th Int. Meet. Lithium Batteries, Münster, Germany, 10–15 May, 1992*.